Layered Hydroxide Metal Acetates (Metal = Zinc, Cobalt, and Nickel): Elaboration via Hydrolysis in Polyol Medium and Comparative Study

Laurence Poul, Noureddine Jouini,* and Fernand Fiévet

Laboratoire de Chimie des Matériaux Divisés et Catalyse, Université Paris VII, 2, place Jussieu, 75251 Paris Cedex 05, France

Received November 18, 1999. Revised Manuscript Received July 31, 2000

Layered hydroxide metal acetates (metal = zinc, cobalt, and nickel) have been prepared by a new route belonging to the *chimie douce* method. This novel method involves the hydrolysis, in polyol medium, of in situ-formed complexes supposed to be alkoxyacetates. These layered hydroxide metal acetates present poorly ordered character, and their X-ray patterns have features typical of lamellar compounds with turbostratic disorder. Their chemical formula was established to be $M(OH)_{2-x}(CH_3COO)_x \cdot nH_2O$ with $(x, n) = (0.42, 0.31)$, (0.38, 0.53), and (0.40, 0.63) for Zn, Co, and Ni, respectively. The layered hydroxide nickel acetate has a classical brucite structure with a random substitution of some hydroxyl groups by acetate groups. The layered hydroxide zinc and cobalt acetates are isomorphous with the hydrozincite structure, in which cations are located in both octahedral and tetrahedral sites. The acetate anion behaves as a unidentate ligand in LHS−Ni and LHS−Co, where LHS indicates layered hydroxide salt, and is intercalated as a free anion in the zinc compound. The dehydration is a reversible topotactic process for LHS−Ni and Co, whereas it is a destructive process in the case of LHS−Zn.

Introduction

Several works in the past decade[1−5] have shown that a great variety of inorganic compounds (metal, oxides) can be easily obtained in polyols because of numerous properties of such solvents, including high boiling point (up to 250 °C) and complexing, reducing, and surfactant properties, in addition to their amphiprotic character.

General principles that emerge from these studies show that the main chemical reactions occurring in polyols are reduction and hydrolysis. Competition between these reactions is easily controlled by adjustment of the hydrolysis ratio. The absence of water favors reduction, leading to micron or submicron metal particles with tailored size and morphology.[6] On the contrary, the presence of water inhibits reduction and enhances hydrolysis, so that the corresponding oxides are obtained via inorganic polymerizations.[7] Molecular precursors subject to these reactions are supposed to be in situ-formed alkoxides or intermediate alkoxy−salt complexes. Such species have clearly been evidenced and structurally characterized for zinc acetate dissolved in diethyleneglycol or ethyleneglycol.[8,9] Therefore, this novel method for elaborating metal oxides can be considered as an intermediate route between the two well-known sol−gel processes that involve hydrolysis reactions of an inorganic salt in aqueous solution or of a metal alkoxide in organic solvent (alcohol).[10]

The aim of this work is two-fold. First, it shows that this novel route can be extended to elaborate layered hydroxide metal acetates (metal = Ni, Co, and Zn), which have, up to now, been prepared in aqueous solution.[11−14] The second goal of this work is to bring new insights into the thermal behavior and morphological and structural features of these materials. Indeed, as will be shown in this paper, the cited previous works have led to incomplete and arguable characterizations. This is because of the poorly crystallized character of such compounds and the limited experimental proofs. We demonstrate here that a more accurate characterization can be obtained by the use of appropriate and complementary techniques: ionic chromatography, temperature-resolved X-ray diffraction and IR spectroscopies,

* Author to whom correspondence should be addressed. E-mail: jouini@ccr.jussieu.fr.

(1) Fiévet, F.; Lagier, J. P.; Figlarz, M. *MRS Bull.* **1989**, *14*, 29.
(2) Silvert, P. Y.; Tekaia-Elhsissen, K. *Solid State Ionics* **1995**, *82*, 53.
(3) Toneguzzo, P.; Viau, G.; Acher, O.; Fiévet-Vincent, F.; Fiévet, F. *Adv. Mater.* **1998**, *10*, 1032.
(4) Collins, I. R.; Taylor, S. E. *J. Mater. Chem.* **1992**, *2*, 1277.
(5) Jézéquel, D.; Guenot, J.; Jouini, N.; Fiévet, F. *J. Mater. Res.* **1995**, *10*, 77.
(6) Fiévet, F.; Lagier, J. P.; Blin, B.; Beaudoin, B.; Figlarz, M. *Solid State Ionics* **1989**, *32/33*, 198.
(7) Poul, L.; Jouini, N.; Fiévet, F. *Congr. Soc. Fr. Chim.* Bordeaux-Talence, **1997**, 318.
(8) Jouini, N.; Poul, L.; Fiévet, F.; Robert, F. *Eur. J. Solid State Inorg. Chem.* **1995**, *32*, 1129.
(9) Poul, L.; Jouini, N.; Fiévet, F.; Herson, P. *Z. Kristallogr.* **1998**, *213*, 416.
(10) Livage, J.; Henry, M.; Jolivet, J. P.; Sanchez, C. *MRS Bull.* **1990**, *15*, 25.
(11) Genin, P.; Delahaye-Vidal, A.; Portemer, F.; Tekaia-Elhsissen, K.; Figlarz, M. *Eur. J. Solid State Inorg. Chem.* **1991**, *28*, 505.
(12) Laget, V.; Rouba, S.; Rabu, P.; Hornick, C.; Drillon, M. *J. Magn. Magn. Mater.* **1996**, *154*, L7.
(13) Kawai, A.; Sugahara, Y.; Park, Y.; Kuroda, K.; Kato, C. *Ceram. Trans.* **1991**, *22*, 75.
(14) Nishizawa, H.; Kishikawa, T.; Minami, H. *J. Solid State Chem.* **1999**, *146*, 39.

10.1021/cm991179j CCC: $19.00
Published on Web 09/23/2000

Table 1. Preparation of Layered Hydroxide Acetate Metal (M = Zn, Co, and Ni)

reactant	conc (M)	solvent	dissolving temp (°C)	h	precipitation temp (°C)
$ZnAc_2{\cdot}2H_2O$	0.5	DEG	130	>2	RT
	0.5	1,2-propanediol	112	>2	RT
	0.1	ethanol	76	>2	RT
$CoAc_2{\cdot}4H_2O$	0.1	DEG	160	≥26	60
	0.1	1,2-propanediol	150	≥26	60
	0.05	ethanol	56	≥26	60
$NiAc_2{\cdot}4H_2O$	0.1	DEG	110	≥4	60
	0.1	1,2-propanediol	140	≥4	60
	0.05	ethanol	61	≥4	60

TG coupled to mass spectrometry analysis, and UV spectroscopy. Furthermore, whereas in previous works these compounds have been separately studied, our comparative investigation evidences significant differences between these three solids despite their similar general characteristics.

It is worth noting that these compounds are of interest in the field of materials. For instance, the hydroxide cobalt and nickel acetates belong to a family of layered compounds showing very interesting magnetic properties.[15−17] In addition, applications in the fields of anionic exchange and electrode materials can be expected.

Experimental Section

Synthesis. The hydrated metal acetates $Zn(CH_3COO)_2{\cdot}2H_2O$, $Co(CH_3COO)_2{\cdot}4H_2O$, $Ni(CH_3COO)_2{\cdot}4H_2O$, polyols [diethyleneglycol (DEG), 1,2-propanediol], and ethanol were purchased from Prolabo and used without any further purification.

The general procedure involves dissolution of an acetate salt in a given volume of polyol (250 mL), followed by addition of water at room temperature (RT) and hydrolysis. The precipitated product is washed several times with ethanol and dried in an oven.

The main factors governing the formation of the desired compounds are the hydrolysis ratio, defined as $h = n\mathrm{H_2O}/n\mathrm{M}$ (M = Ni, Co, Zn), and the metal concentration. The optimal experimental conditions required are listed in Table 1.

As shown in this table, the compounds can be obtained for a large range of hydrolysis ratios. Under the lower limit, the solution remains limpid, and no precipitation is observed. It should be noted that a ratio h equal to 250 (a mixture of 250 mL of polyol and 110 mL of water) for a metal concentration $C = 0.1$ M has been retained to synthesize the studied compounds. This approach will be justified below.

Metal concentrations used in ethanol are low, as salts barely dissolve in this solvent. In the other solvents, nickel and cobalt concentrations higher than 0.1 M led to a mixture of the desired compound and a side phase. For the three metals, the lowest yield was observed for ethanol, and the highest for DEG. Thus, this latter solvent has been retained to elaborate the studied compounds.

Chemical Analysis. Elemental analysis of metal, carbon, and hydrogen was performed at the Vernaison Analysis Centre of CNRS. Zinc, cobalt, and nickel ions were also titrated by EDTA using Eriochrome black T for the two former and alcoholic dithizone for the latter as the indicators. The total base content was estimated by dissolving a known quantity of the sample in an excess of hydrochloric acid and back-titrating the excess of acid against standard sodium hydroxide using a pH meter. The acetate content was determined by ionic chromatography with a DIONEX DX-100 ion chromatograph equipped with AG-4 and AS4−SC columns.

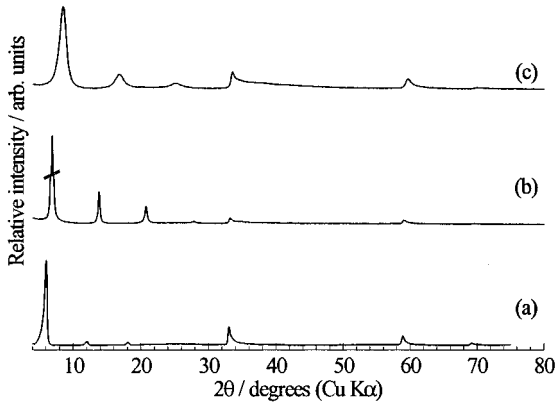

Figure 1. X-ray diffraction patterns of (a) LHS−Zn, (b) LHS−Co, and (c) LHS−Ni (Cu Kα).

Characterization. X-ray diffraction was carried out with two types of diffractometer (a Siemens D5000 diffractometer for RT measurements and a vertical Phillips PW1050 diffractometer, in a Pt−Rh40% sample holder, for temperature-resolved diffraction), in the 2θ range 5−100°, with a step of 0.03°(2θ) and a step duration of at least 17 s.

IR spectra were recorded with a FTIR Perkin-Elmer 1750 spectrophotometer in transmittance mode between 4000 and 500 cm^{-1} with a resolution of 4 cm^{-1} and with at least 20 acquisitions. The samples were prepared in KBr pellets. Temperature-resolved IR spectroscopy was performed in diffuse reflectance mode under nitrogen in a Harrick praying mantis apparatus.

Differential thermal and thermogravimetric analyses (DTA and TGA) were carried out with a heating rate of 1 °C min^{-1} in an alumina crucible under oxygen in a Setaram TG92−12 thermal analyzer. Thermal analysis (Setaram balance TG DSC111) coupled with mass spectrometric analysis (Leybold Inficom H 300 CIS spectrometer) were carried out under argon up to 700 °C in a platinum crucible with a heating rate of 5 °C min^{-1}.

UV−visible−NIR diffuse reflectance spectra were recorded between 200 and 2500 nm on a Cary 5E spectrophotometer equipped with an integration sphere coated with pressed polytetrafluoroethylene (PTFE).

Electron microscopy and diffraction studies were conducted on a JEOL-100 CX II microscope.

Results

X-Ray and Morphological Characterizations. Regardless of the solvent used (DEG, 1,2-propanediol, or ethanol), the X-ray diffraction patterns show the formation of the same compound for a given metal with almost identical interlayer distances. All of the X-ray patterns have features typical of incompletely ordered lamellar compounds related to the brucite structure (Figure 1): sharp reflections in the range of small Bragg angles and broad and asymmetric reflections in the range of high angles. Such features can be explained on the basis of stacking order of brucite-like sheets parallel and equidistant but twisted and/or translated against each other. This turbostratic behavior has been observed for α-$Ni(OH)_2$, for α-$Co(OH)_2$,[18−20] and for the

(15) Laget, V.; Hornick, C.; Rabu, P.; Drillon, M.; Turek, P.; Ziessel, R. *Adv. Mater.* **1998**, *10*, 1024.
(16) Kurmoo, M. *Chem. Mater.* **1999**, *11*, 3370.
(17) Kurmoo, M.; Day, P.; Derory, A.; Estournès, C.; Poinsot, R.; Stead, M. J.; Kepert, C. J. *J. Solid State Chem.* **1999**, *145*, 452.
(18) Le Bihan, S.; Figlarz, M. *J. Cryst. Growth* **1972**, *13/14*, 458.
(19) Ismail, J.; Ahmed, M. F.; Kamath, P. V.; Subbanna, G. N.; Uma, S.; Gopalakrishnan, J. *J. Solid State Chem.* **1995**, *114*, 550.
(20) Dixit, M.; Subbanna, G. N.; Kamath, P. V. *J. Mater. Chem.* **1996**, *6*, 1429.

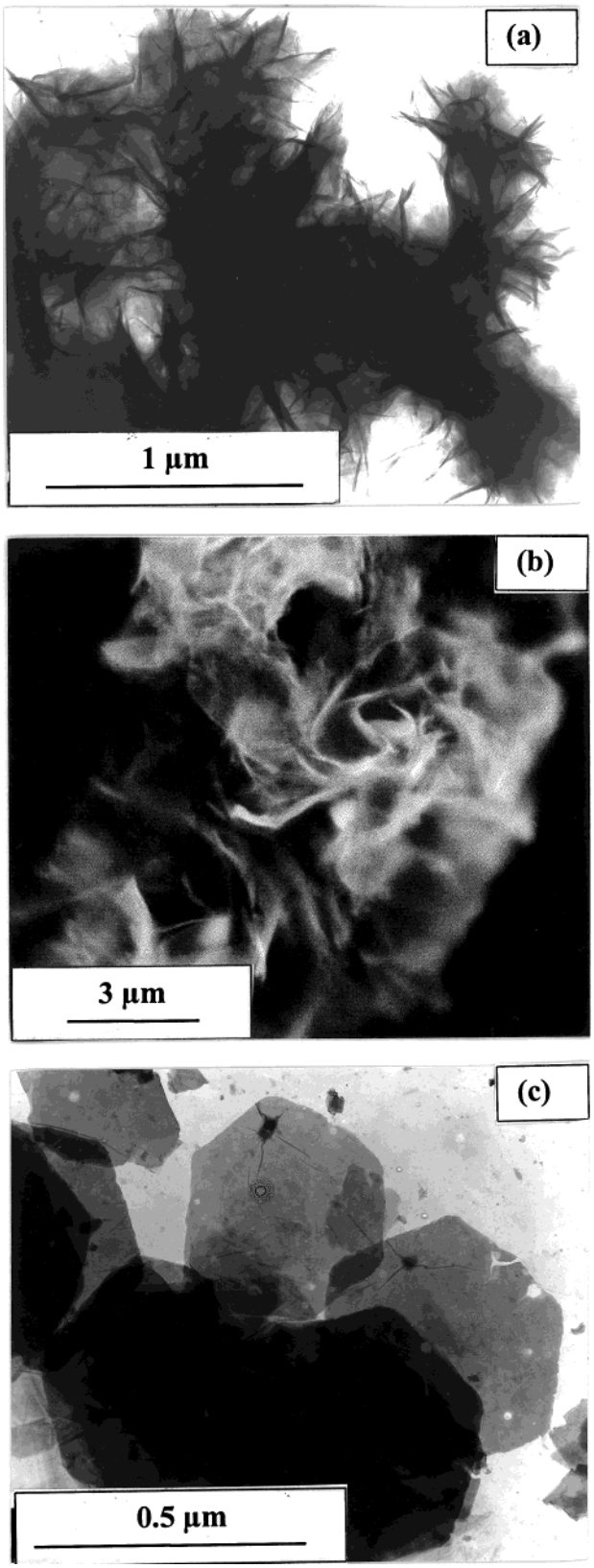

Figure 2. TEM micrographs of (a) LHS−Ni, (b) LHS−Zn, and (c) LHS−Co.

relatively wide family of layered double hydroxides (LDH) $[M^{2+}_{1-x}M'^{3+}_{x}(OH)_2]^{x+}[A^{m-}_{x/m}\cdot nH_2O]$.[21] Similarly, the studied compounds will be called layered hydroxide salts (LHSs) and refered to as LHS−M (M = Ni, Co, and Zn).

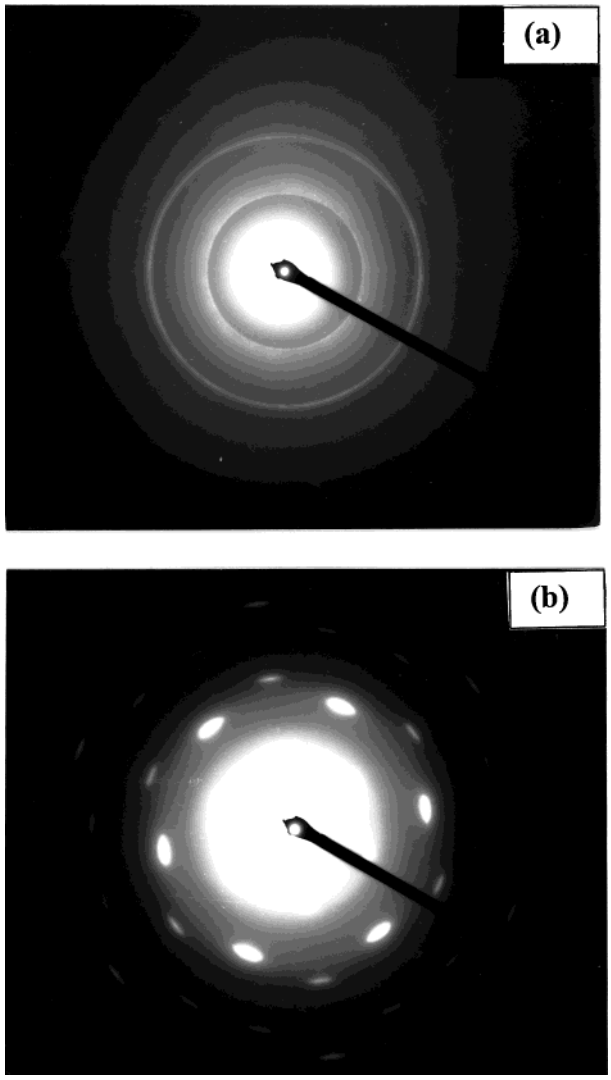

Figure 3. Electron diffraction patterns of (a) LHS−Ni and (b) LHS−Co.

Electron microscopy reveals significantly different morphologies for the three LHSs (Figure 2). On one side, LHS−Ni and LHS−Zn exhibit characteristic features of turbostratic materials: they appear as aggregates of thin crumpled sheets without any definite shape. LHS−Zn decomposes under electron beam, and LHS−Ni gives a pattern of rings (Figure 3 a) corresponding to *hk*0 reflections. LHS−Co is significantly more crystallized. It consists of an aggregate of thin hexagonal platelike particles with a diameter close to 0.5 μm. Electron diffraction shows that hexagonal platelets are mono crystals lying on the (00*l*) plane, as all observed reflections can be explained as *hk*0 reflections (Figure 3b). This unexpected morphology has been observed for a blue cathodically deposited cobaltous hydroxide, α-$Co(OH)_2$.[22]

The X-ray patterns have been indexed in the hexagonal system (Table 2), in agreement with electron microscopy results discussed above and general predictions of X-ray patterns of turbostratic materials.[23] Sharp

(21) Cavani, F.; Trifiro, F.; Vaccari, A. *Catal. Today* **1991**, *11*, 173.

(22) Benson, P.; Briggs, G. W. D.; Wynne-Jones, W. F. K. *Electrochim. Acta* **1964**, *9*, 281.

Table 2. Cell Parameters and X-ray Diffraction Patterns of LHS−M (M = Zn, Ni, and Co)

	M = Zn			M = Co			M = Ni		
a (Å)	3.138(1)			3.118(2)			3.106(3)		
c (Å)	14.75(1)			12.84(2)			10.64(3)		
hkl	d_{obs} (Å)	d_{calc} (Å)	I_{rel}	d_{obs} (Å)	d_{calc} (Å)	I_{rel}	d_{obs} (Å)	d_{calc} (Å)	I_{rel}
0 0 1	14.68	14.75	100	12.90	12.84	100	10.54	10.64	100
0 0 2	7.36	7.38	5	6.43	6.42	12	5.30	5.32	19
0 0 3	4.91	4.92	4	4.29	4.28	7	3.55	3.55	6
0 0 4	–	–	–	3.211	3.211	1	–	–	–
1 0 0	2.717	2.718	24	2.700	2.701	12	2.680	2.690	19
1 1 0	1.569	1.569	13	1.560	1.559	8	1.553	1.553	13
2 0 0	1.359	1.359	3	–	–	–	1.346	1.345	1

Table 3. Calculated and Observed Chemical Results for LHS−M (M = Zn, Ni, and Co)

		Ac/M	%M		%C		%H		% mass loss	
compound	formula	exp	exp	calc	exp	calc	exp	calc	exp (ATG)	calc
LHS−Zn	$Zn(OH)_{1.58}(Ac)_{0.42}\cdot 0.31H_2O$	0.42	51.78	53.32	9.27	8.22	2.69	2.82	32.15	33.62
LHS−Co	$Co(OH)_{1.62}(Ac)_{0.38}\cdot 0.53H_2O$	0.38	48.00	49.76	9.05	7.70	3.26	3.23	31.90	32.23
LHS−Ni	$Ni(OH)_{1.60}(Ac)_{0.40}\cdot 0.63H_2O$	0.40	46.53	48.58	9.55	7.94	3.26	3.36	39.14	38.18

reflections were explained as 00*l*, and asymmetric reflections as *hk*0. The parameters in the basal plane that represent the metal−metal distances are very close to those of the corresponding β-$M(OH)_2$ compounds (for M = Zn, Co, and Ni, d_{M-M} = 3.194, 3.173, and 3.114 Å, respectively).[24−26]

The 00*l* reflection broadening for LHS−Ni is higher than that for the two other compounds. The crystallite mean size along the *c* axis (50 Å) inferred from the Scherrer formula corresponds to a very small number of layers per crystallite: 5 compared to about 15 layers for LHS−Zn and 50 layers for LHS−Co.

Chemical Analysis and Formula. Results obtained from chemical analysis, acido-basic titration, and ionic chromatography (analysis of acetate ion) are summarized in Table 3.

The observed carbon amount is higher than that due to acetate deduced from ionic chromatography. This shows that polyol is still present in the as-synthesized compounds**.** Two types of interaction can occur: a physical adsorption on the external surface of particles or an intercalation of polyol between the layers, as was observed in earlier works.[27,28]

Despite the bidimensional character of the hydroxyacetates that are the object of this work, X-ray patterns of the compounds obtained in different solvents clearly show that variations in the nature of the polyol have no effect on the interlamellar distance, which remains constant for a given cation. Furthermore, work in ethanol led to X-ray patterns identical to those obtained in polyol. Accordingly, it appears that the solvent is only adsorbed on the external surface of the crystallites. It should be noted that the amount of adsorbed polyol depends on the hydrolysis ratio. It is as low as 0.03, 0.04, and 0.05 mol of polyol per 1 mol of Zn, Co, and Ni, respectively, when h = 250.

The water amount in the formulation was deduced by subtracting the mass of metal, hydroxide, acetate, and polyol from the total mass. Chemical formulas inferred from these results are also reported in Table 3.

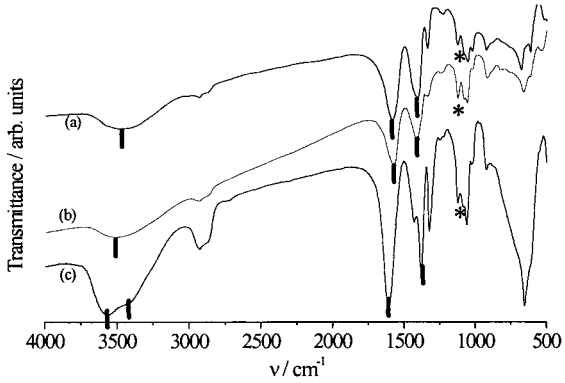

Figure 4. IRFT spectra at room temperature of (a) LHS−Zn, (b) LHS−Co, and (c) LHS−Ni (* = adsorbed polyol)

The observed total loss was deduced from TGA. The agreement between expected and observed results can be deemed satisfactory if one considers the amount of adsorbed solvent.

Infrared Study. Infrared studies confirm the composition established by chemical and TG−mass spectrometric investigations. They clearly show the presence of acetate, hydroxyl, and water species.

For each compound (Figure 4), at least two bands are observed in the range 1600−1300 cm^{-1}: at 1583 and 1411 cm^{-1} for Zn and at 1572 and 1417 cm^{-1} for Co. For Ni, in addition to the two intense bands at 1614 and 1381 cm^{-1}, a third band is observed at 1431 cm^{-1}. If we omit the latter band, which may be due to CH_3 deformation,[29] the two bands observed for each compound are the fingerprint of the acetate group. Indeed, the bands ν_{as} and ν_s of C=O in acetate group lie in the ranges 1620−1570 and 1430−1300 cm^{-1}, respectively.[30]

The temperature-resolved IR study reveals that the difference $\Delta\nu = \nu_{as} - \nu_s$ increases from 227 and 163 cm^{-1} to 255 (at 250 °C) and 220 cm^{-1} (at 200 °C) for LHS−

(23) Yang, D.; Frindt, R. F. *J. Mater. Res.* **1996**, *11*, 1733.
(24) Baneyeva, M. I.; Popova, S. V. *Geochem. Int.* **1969**, *6*, 807.
(25) Lotmar, W.; Feitknecht, W. *Z. Kristallogr.* **1936**, *93*, 368.
(26) Cairns, R. W.; Ott, E. *J. Am. Chem. Soc.* **1933**, *55*, 527.
(27) Benes, L.; Melanova, K.; Zima, V.; Votinsky, J. *J. Solid State Chem.* **1998**, *141*, 64.
(28) Tekaia-Elhsissen, K.; Delahaye-Vidal, A.; Nowogrocki, G.; Figlarz, M. *C. R. Acad. Sci. Paris* **1989**, *309*, 469.
(29) Alcock, N. W.; Tracy, V. M.; Waddington, T. C. *J. Chem. Soc., Dalton Trans.* **1976**, 2243.
(30) Nakamoto, K. *Infrared and Raman Spectra of Inorganic and Coordination Compounds*, 4th ed.; Wiley: New York, 1986.

Table 4. Evolution of Δν with Temperature for LHS−M (M = Zn, Ni, and Co)

M = Zn				M = Co				M = Ni			
T (°C)	ν_{as}(C−O) (cm^{-1})	ν_s(C−O) (cm^{-1})	Δν (cm^{-1})	T (°C)	ν_{as}(C−O) (cm^{-1})	ν_s(C−O) (cm^{-1})	Δν (cm^{-1})	T (°C)	ν_{as}(C−O) (cm^{-1})	ν_s(C−O) (cm^{-1})	Δν (cm^{-1})
20	1583	1411	172	20	1569	1406	163	20	1609	1379	227
50	1581	1409	172	110	1579	1387	192	50	1616	1375	241
80	1579	1408	171	170	1594	1381	213	130	1620	1369	251
110	1579	1407	172	200	1598	1378	220	190	1620	1368	252
								250	1620	1365	255

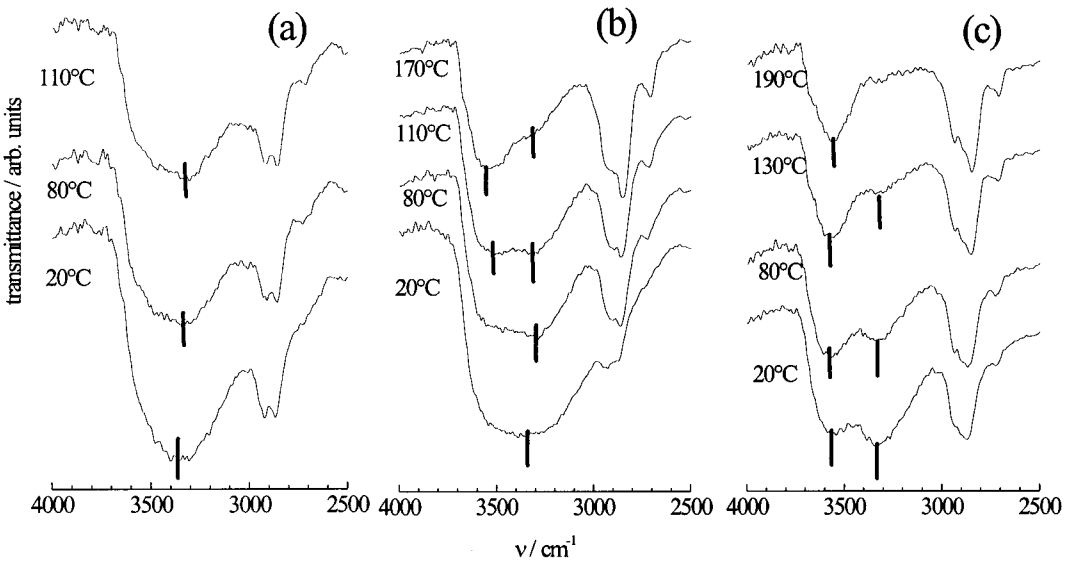

Figure 5. Temperature-resolved IRFT spectra of (a) LHS−Zn, (b) LHS−Co, and (c) LHS−Ni, in the range of 4000−2500 cm^{-1}.

Ni and LHS−Co, respectively, in the temperature range corresponding to the thermal stability of these compounds. For the LHS−Zn compound, this difference (172 cm^{-1}) remains almost constant upon heating (Table 4).

Hydroxyl groups and water are evidenced by the broad bands observed at high frequency, at 3350 and 3400 cm^{-1} for Zn and Co, respectively, and by two broad bands at 3323 and 3553 cm^{-1} for Ni. The broadening of these bands is due to hydrogen bond formation.[31,32] In fact, for Co, the broad adsorption band became resolved into at least two components when the temperature was increased. Lower frequency bands at 3400 and 3323 cm^{-1} for Co and Ni, respectively, correspond to interlamellar water, as these bands disappeared upon dehydration, as shown in temperature-resolved IR spectra (Figure 5b,c) and as already attributed in the case of α-Ni(OH)$_2$.[33] This dehydration step is clearly identified from the TG and mass spectrometric analyses. The band at higher frequency is due to the hydroxyl group of the brucite-like layer. For Zn, the band at 3350 cm^{-1} remains unresolved upon heating (Figure 5a). The expected band (1600 cm^{-1}) arising from the bending mode δH_2O is obscured by the strong band at 1500−1600 cm^{-1} due to the C═O asymmetric stretching mode, as observed in previous works on hydrated metal acetates[34] and $Cu_2(OH)_3(CH_3COO)\cdot H_2O$.[35]

Polyol infrared bands in the range 1200−1000 cm^{-1} (indicated by * on the spectra) can also be detected in the spectra without any shift or splitting compared to pure polyol bands. This confirms that polyol is present as a neutral adsorbed species.

Thermal Evolution. *Thermal Analysis.* Figure 6 represents thermogravimetric and differential thermal analyses (TGA and DTA) conducted under oxygen. Chemical species evolved during thermal treatment have been identified by TGA coupled to mass spectrometry. X-ray diffraction patterns show that the final products of decomposition are NiO, Co_3O_4, and ZnO. Ni and Co compounds have similar thermal behaviors. A first loss due to the departure of water occurs around 60 °C and corresponds to a broad endothermic peak. A second weight loss is observed at higher temperature in the ranges 240−285 °C and 180−240 °C for the Ni and Co compounds, respectively, and corresponds to exothermic peaks. It involves formation of water and CO_2 through the dehydroxylation reaction and combustion of acetate anions. This combustion with a strong exothermic effect probably corresponds to a catalytic oxidation of acetate caused by the presence of Ni and Co oxides.

For Zn, two losses with endothermic peaks are observed. The first loss, at around 90 °C, is due to the departure of intercalate water. The second, at around 120 °C, corresponds to the release of water concomitantly with the dehydroxylation of the layers. A third loss, in the range 250−300 °C, corresponds to the departure of CO_2 through a slow decomposition of the acetate group.

This difference will be discussed later in relation to structural characteristics.

(31) Kooli, F.; Chisem, I. C.; Vucelic, M.; Jones, W. *Chem. Mater.* **1996**, *8*, 1969.
(32) Labajos, F. M.; Rives, V.; Ulibarri, M. A. *J. Mater. Sci.* **1992**, *27*, 1546.
(33) Le Bihan, S. Ph.D. Thesis. Etude d'un hydroxyde de nickel à organisation cristalline imparfaite: structure et propriétés. Université Paris VI, 1974.
(34) Baraldi, P.; Fabbri, G. *Spectrochim. Acta* **1981**, *37A*, 89.
(35) Masciocchi, N.; Corradi, E.; Sironi, A.; Moretti, G.; Minelli, G.; Porta, P. *J. Solid State Chem.* **1997**, *131*, 252.

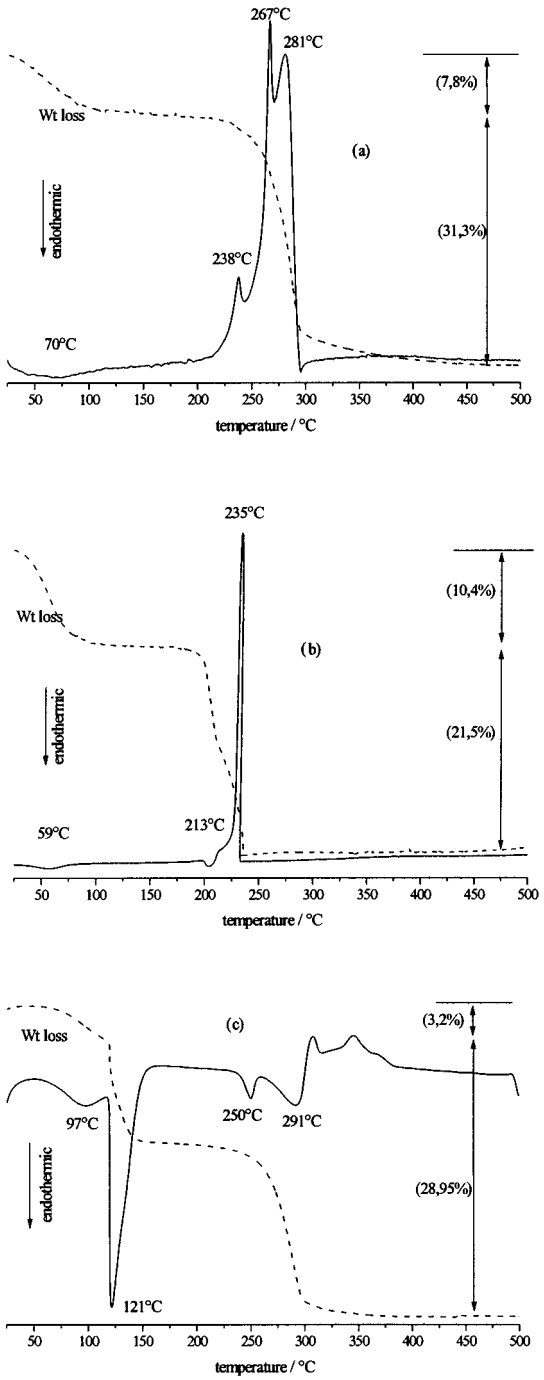

Figure 6. TGA and DTA curves of (a) LHS−Ni, (b) LHS−Co, and (c) LHS−Zn under oxygen.

Temperature Resolved X-ray Diffraction. When heated, LHS−Co and LHS−Ni on one side and LHS−Zn on the other side exhibit different behavior (Figure 7a−c, respectively). For LHS−Co and LHS−Ni, the 00*l* reflections decrease in intensity and become more diffuse, suggesting disorder in the stacking of layers, and the corresponding interlamellar distances collapse from 12.9 and 10.5 Å to 10.2 and 8.2 Å, respectively. This collapse is due to the departure of water, as was shown by the analysis of TGA coupled to mass spectrometry. Conversely, the *hk*0 distances remain almost constant. The decomposition of the Ni and Co compounds occurred, respectively, at 290 and 230 °C, leading to finely divided NiO and Co_3O_4 according to their very broad diffraction peaks.

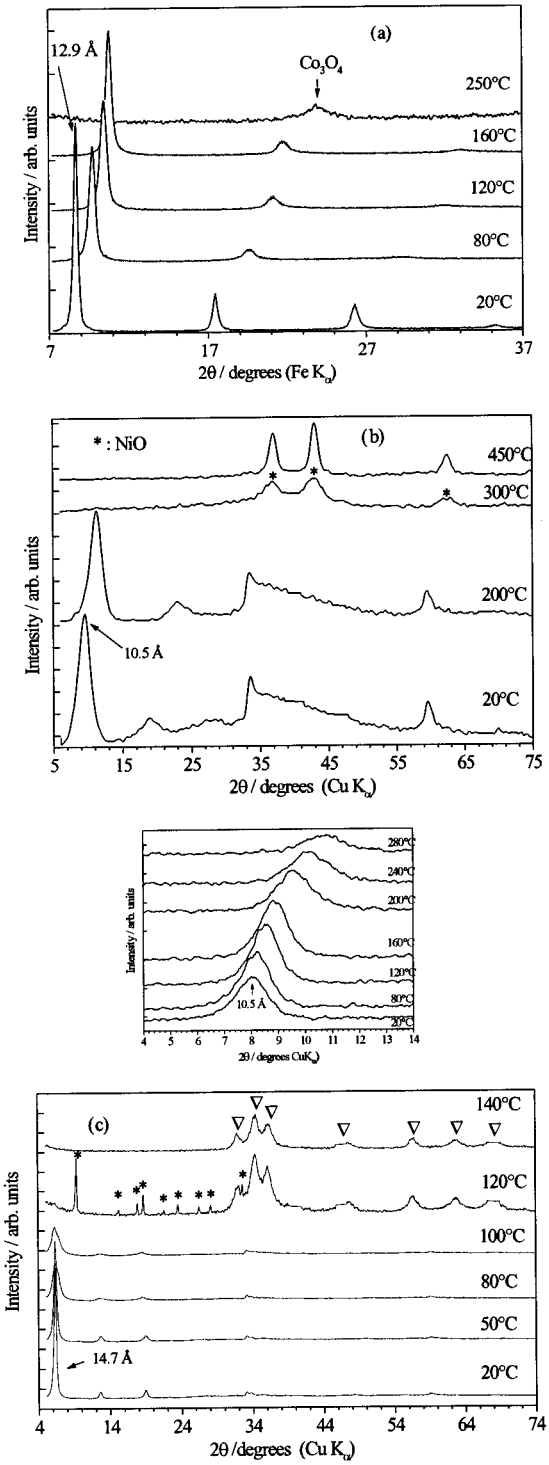

Figure 7. Temperature-resolved X-ray diffraction patterns of (a) LHS−Co (Fe K_α), (b) LHS−Ni and evolution of the distance 001 (Cu K_α), and (c) LHS−Zn (* = zinc oxide, ▽ = zinc oxoacetate) (Cu Kα).

For LHS−Zn, the 00*l* distances remain constant upon heating, but their intensities become weaker and more diffuse until destruction of the compound at a relatively low temperature (120 °C). The analysis of TGA coupled to mass spectrometry showed that this decomposition is due to the departure of water, including that due to the dehydroxylation process. Indeed, this decomposition leads to the formation of a mixture of zinc oxide and a second phase identified as a zinc oxoacetate by Golgotiu et al.[36] This phase undergoes a transformation at higher

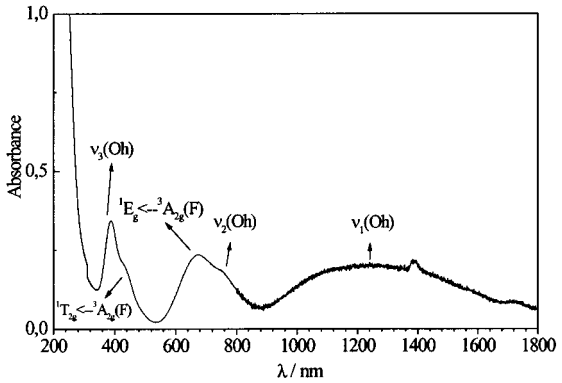

Figure 8. UV−visible spectra of LHS−Ni.

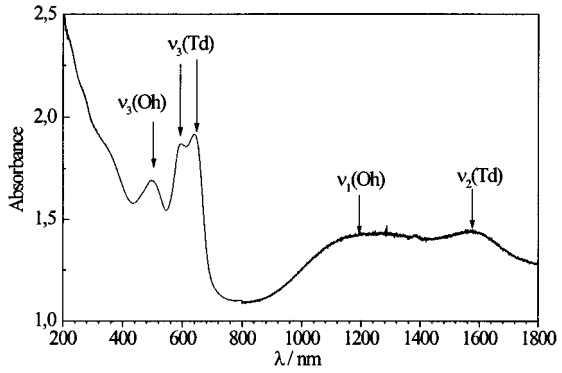

Figure 9. UV−visible spectra of LHS−Co.

Table 5. Energies and Assignments of Bands Observed in the UV−Vis Spectra of LHS−M (M = Ni and Co)

compound	transition energy (cm^{-1})	assignment	symmetry
LHS−Ni	8064	ν_1: $^3T_{2g}(F) \leftarrow {}^3A_{2g}(F)$	O_h
	13141	ν_2: $^3T_{1g}(F) \leftarrow {}^3A_{2g}(F)$	
	14903	$^1E_g(G) \leftarrow {}^3A_{2g}(F)$	
	22747	$^1T_{1g}(G) \leftarrow {}^3A_{2g}(F)$	
	25840	ν_3: $^3T_{1g}(P) \leftarrow {}^3A_{2g}(F)$	
LHS−Co	6382	$\nu_2{}^{T_d}$: $^4T_1(F) \leftarrow {}^4A_2(F)$	T_d
	8267	$\nu_1{}^{O_h}$: $^4T_{2g}(F) \leftarrow {}^4T_{1g}(F)$	O_h
	15596 and 16883	$\nu_3{}^{T_d}$: $^4T_1(P) \leftarrow {}^4A_2(F)$	T_d
	20267	$\nu_3{}^{O_h}$: $^4T_{1g}(P) \leftarrow {}^4T_{1g}(F)$	O_h

temperature that leads to zinc oxide.

Hydration−dehydration appears to be a reversible process for LHS−Co and LHS−Ni. Upon exposure to moist air, dehydrated LHS−Co transformed into hydrated form more rapidly (90 min) than LHS−Ni (48 H).

UV−Visible−NIR Reflectance Spectroscopy. The UV−visible spectra of the compounds are shown in Figures 8 and 9. Energies and assignments of the observed bands are given in Table 5.

The nickel compound spectrum shows weak d−d absorption corresponding to Ni(II) in octahedral coordination of a weak ligand. The crystal field strength Δ_{O_h} deduced (8172 cm^{-1}) (the average value obtained from Δ_{O_h} for ν_1 and ν_2) is close to the value for β-Ni(OH)$_2$ (Δ_{O_h} = 8600 cm^{-1}) and the Racah parameter B = 1041 cm^{-1} is in the same range as that observed for β-Ni(OH)$_2$, B = 820−925 cm^{-1}.[37]

The cobalt compound spectrum shows d−d absorption corresponding to Co(II) in octahedral coordination and two additional sharp peaks at lower energies due to Co(II) in a tetrahedral coordination geometry. The crystal field strength values (Δ_{O_h} = 10 334 cm^{-1} and Δ_{T_d} = 3545 cm^{-1}), calculated, respectively, with $\nu_1(O_h)$ and $\nu_2(T_d)$ and the Racah parameters (B_{O_h} and B_{T_d}, respectively, 938 and 756 cm^{-1}) are in good agreement with those given in the literature (Δ = 9200 cm^{-1} and B = 825 cm^{-1} for $[Co(OH_2)_6]^{2+}$ [38] and Δ = 3900 cm^{-1} and B = 775 cm^{-1} for ZnO:Co[39]).

Discussion

A New Preparative Route: Hydrolysis in Polyol Medium. To date, LHS compounds have been prepared via two main routes conducted in aqueous media: partial basic titration at RT and hydrolysis, at elevated temperature under hydrothermal conditions, of a metal salt solution or exchange reactions. Our work describes a new method, not yet reported in the literature, for preparing such materials. This novel route belongs to the general *chimie douce* method and is closely related to the sol−gel process. It involves several steps, including the dissolution of metal acetate in polyol medium and the in situ formation of complexes (supposed to be alkoxyacetates), which are then hydrolyzed. This novel route is very attractive and offers several advantages. When the work is performed in polyol medium, the precipitation of the hydroxyacetates is easily controlled through adjustments in the hydrolysis ratio for a ratio of acetate/metal equal to 2. In the aqueous method, this step requires a very careful control of the pH by partial titration with NaOH. Furthermore, for LHS−Ni, the synthesis in aqueous solution led to a contamination with carbonate anion. Avoidance of this contamination requires synthesis under hydrothermal conditions at 160 °C. In polyol medium, this is achieved more easily at 60 °C and under atmospheric condition. As has been suggested by Hansen et al., polyols can react with carbonate, leading to the release of CO_2.[40]

Structural Characteristics. Table 6 allows the studied compounds to be compared to similar compounds prepared in aqueous solution.

The two routes led to compounds with similar formulas if we omit the very low amount of carbonate in the LHS−Ni prepared in aqueous medium and the high amount of water for the LHS−Ni obtained under hydrothermal conditions. However, their physical characteristics appear to be slightly different. Interlamellar distances are higher for LHS−Zn and LHS−Ni prepared in polyol than for the corresponding compounds elaborated in aqueous solution. The $\Delta\nu$ values [$\Delta\nu = \nu_{as}(CO) - \nu_s(CO)$] are also different.

X-ray patterns of the three solids are similar to those observed for layered compounds with brucite[41] or hydrozincite[42] structures. Brucite can be described as a packing of single layers consisting of $Mg(OH)_6$ edge-sharing octahedra, the cohesion between layers being

(36) Golgotiu, T.; Rosca, I. *Bul. Inst. Politeh. Iasi* **1969**, *XV(XIX)*, 1.
(37) Minkova, N.; Krusteva, M.; Nikolov, G. *J. Molec. Struct.* **1984**, *115*, 23.
(38) Lever, A. B. P. *Inorganic Electronic Spectroscopy*; Elsevier: New York, 1984.
(39) Weakliem, H. A. *J. Chem. Phys.* **1961**, *36*, 2117.
(40) Hansen, H. C. B.; Taylor, R. M. *Clay Miner.* **1991**, *26*, 311.
(41) Aminoff, G. *Z. Kristallogr.* **1921**, *56*, 505.
(42) Ghose, S. *Acta Crystallogr.* **1964**, *17*, 1051.

Table 6. Characteristics of LHS−M (M = Zn, Co, Ni) Prepared in Polyol and Aqueous Media

compound	formula	interlamellar distance (Å)	$\Delta\nu$ (cm^{-1}) ($\nu_{as} - \nu_s$)	ref
LHS−Zn	$Zn(OH)_{1.58}(Ac)_{0.42}\cdot 0.31H_2O$	14.68	172	this work
	$Zn(OH)_{1.60}(Ac)_{0.40}\cdot 0.60H_2O$	13.8	195	13
LHS−Co	$Co(OH)_{1.62}(Ac)_{0.38}\cdot 0.53H_2O$	12.90	163	this work
	$Co(OH)_{1.50}(Ac)_{0.50}\cdot 0.50H_2O$	12.8	−	12
LHS−Ni	$Ni(OH)_{1.60}(Ac)_{0.40}\cdot 0.63H_2O$	10.54	230	this work
	$Ni(OH)_{1.55}(Ac)_{0.43}(CO_3)_{0.01}\cdot 0.20H_2O$	9.3	180	11
	$Ni(OH)_{1.5}(Ac)_{0.5}\cdot 1.4H_2O$	9.44	208	14

assured by van der Waals forces. β-$M(OH)_2$ compounds (M = Ni, Co, and Zn) belong to this structural type. The hydrozincite structure has the form of an inorganic triple-layer slab. Indeed, in this structure, a brucite sheet, in which one-quarter of the cation sites are vacant, is sandwiched between two layers formed by two tetrahedral zinc layer sheets placed above and below each octahedral vacant site. This triple-layer slab type is encountered in zinc hydroxychloride $Zn_5(OH)_8Cl_2\cdot 1H_2O$[43] and hydroxnitrate $Zn_5(OH)_8(NO_3)_2\cdot 2H_2O$.[44] However, these two compounds differ by the nature of the organization of the chemical species in the interlamellar space. For $Zn_5(OH)_8(NO_3)_2\cdot 2H_2O$, the tetrahedral fourth apex pointing into the interlayer space is occupied by the oxygen of a water molecule with nitrate being intercalated in the gallery as a free ion. For $Zn_5(OH)_8Cl_2\cdot H_2O$, chloride ion occupies the fourth apex, and water forms a layer in the interlamellar space. To show both coordinations, these formulas can be written as $[(Zn^{octa})_{1-x}(Zn^{tetra})_{2x}(OH)_2]^{+2x}\cdot 2x(A^-)\cdot nH_2O$ with $x = 0.25$, the anion-to-metal ratio being equal to 0.4.

The comparative study conducted here reveals that the hydroxyacetates of Ni, Co, and Zn, despite their similar X-ray patterns and general chemical formula, present significant structural differences, which concern mainly the cation coordination concomitantly with the thickness of the inorganic layer (single or triple layers) and the organization of the chemical species (water molecule, acetate anion) in the gallery. These two points will be discussed hereafter.

Cation Distribution and Nature of the Layers. UV characterization shows that the nickel ion is exclusively in an octahedral coordination. This indicates that the inorganic sheets in LHS−Ni are constituted by single layers as in β-$Ni(OH)_2$.

In the case of LHS−Co and LHS−Zn, the stacking of single layers is insufficient to account for the high interlamellar distances observed in comparison with those of LHS−Ni.

For LHS−Co, UV analysis shows qualitatively the occurrence of Co^{2+} in both octahedral and tetrahedral sites. The absorption bands of the Co^{T_d}, about a hundred times more intense than the octahedral absorption band, excludes any quantitative determination of the ratio Co^{T_d}/Co^{O_h} by this method.[45] However, this qualitative result, along with the relatively high interlamellar distance (12.9 Å) and the observed acetate/metal ratio (0.4), is consistent with a structural model with triple-layer slabs, such as observed for $Zn_5(OH)_8Cl_2\cdot 1H_2O$ and $Zn_5(OH)_8(NO_3)_2\cdot 2H_2O$. This conclusion is in qualitative agreement with that reached by Laget et al.[12] for LHS−Co prepared in aqueous solution, with, however, the slightly different formula $[(Co^{octa})_{1-x}(Co^{tetra})_{2x}(OH)_2]^{+2x}\cdot 2x(Ac^-)\cdot nH_2O$ with $x = 0.16$.

In LHS−Zn, zinc cations have been found in both tetrahedral and octahedral coordinations. Indeed, starting from LHS−Zn, we have exchanged the acetate anion by chloride and nitrate and recovered the $Zn_5(OH)_8Cl_2\cdot 1H_2O$ and $Zn_5(OH)_8(NO_3)_2\cdot 2H_2O$ homologues whose structures were described earlier. It should be noted that the inverse exchange is also possible. Indeed, Kawai et al. elaborated the LHS−Zn compound by solid/liquid exchange between $Zn_5(OH)_8Cl_2\cdot 1H_2O$ and zinc acetate solution[13] and accordingly concluded that LHS−Zn is isostructural with the hydroxychloride. As for LHS−Co, the Zn compound appears to be formed by inorganic triple-layer slabs, in agreement with the high interlamellar distance observed (14.7 Å).

Interlamellar Organization and Structural Model. Regardless of the temperature (up to 280 °C), LHS−Ni elaborated in polyol presents a $\Delta\nu$ value higher than 200 cm^{-1}. This indicates a unidentate character for the acetate anion according to Nakamoto rules.[30] Such character is consistent with a structural model in which nickel ions are in an octahedral environment forming brucite-like layers. Twenty percent of the anion sites are occupied by acetate species, with the remaining sites being occupied by hydroxyl groups. A very recent work[14] suggested a similar character for the acetate anion for LHS−Ni prepared under hydrothermal conditions. However, our model is in contradiction with two other models proposed in the literature. The first model[11] derives from the brucite structure by the occurrence of vacancies in hydroxyl sites, thus giving a cationic sheet $[M(OH)_{2-x}\square_x]^{+x}$. Electrical neutrality is fulfilled by intercalation of acetate and carbonate anions along with water between the layers. This model is based on Nakamoto rules, which predict a free character for acetate ion that shows a $\Delta\nu$ value less than 200 cm^{-1}. Such a conclusion is subject to discussion because several works have shown that $\Delta\nu$ may be lowered when the acetate ions are engaged in hydrogen bonds. This was clearly demonstrated for $Cu_2(OH)_3(CH_3COO)\cdot H_2O$[35] for which structural determination has shown that the acetate has a unidentate character despite a $\Delta\nu$ value of 140 cm^{-1}. Another model has been invoked, with no experimental proof, to explain the positive charge of the sheets in α-hydroxides.[46] It consists of partial protonation of the hydroxyl groups according to the equilibrium $M(OH)_2 + xH^+ \Leftrightarrow [M(OH)_{2-x}(H_2O)_x]^{+x}$, with anions still intercalated as free ions between the layers.

(43) Allmann, R. *Z. Kristallogr.* **1968**, *126*, 417.
(44) Stahlin, W.; Oswald, H. R. *Acta Crystallogr.* **1970**, *B26*, 860.
(45) Knetsch, D.; Groeneveld, W. L. *Inorg. Chim. Acta* **1973**, *7*, 81.
(46) Kamath, P. V.; Therese, G. H. A.; Gopalakrishnan, J. *J. Solid State Chem.* **1997**, *128*, 38.

Our study evidences for the first time the role of water in the organization of the interlamellar space. When the temperature is increased from RT to 280 °C, a decrease in the lamellar distance by 2.6 Å (from 10.5 to 8.20 Å) is observed. This variation corresponds to the water van der Waals diameter[47] and thus indicates that this chemical species is intercalated as a molecular layer (Figure 10a). Dehydration is confirmed by the disappearance of the broad band at 3323 cm^{-1} in the IR spectra, by the mass spectral analysis, and by the increase in $\Delta\nu$ of the acetate anions because of the breaking of hydrogen bonds. It should be noted that this study shows that LHS−Ni undergoes a topotactic dehydration process that conserves the lamellar character.

Although LHS−Co and LHS−Zn belong to the hydrozincite structural type, temperature-resolved IR and X-ray studies revealed significant differences in the organization of chemical species between the layers.

In LHS−Co, this organization is similar to that observed for LHS−Ni. Indeed, the increase in $\Delta\nu$ from 163 to 220 cm^{-1} (at 200 °C) upon dehydration shows clearly the unidentate character of acetate. Furthermore, when the temperature is increased from RT to 280 °C, a decrease in the lamellar distance by 2.6 Å is observed, indicating that water forms a monolayer. These characteristics are clearly established for the first time. In the work of Laget et al.,[12] the acetate character was supposed to be unidentate without experimental proof, and the role of water was not discussed. Our results indicate that LHS−Co is isostructural with zinc hydroxychloride, with the anion acetate in the tetrahedral coordination of Co and water intercalated as monolayer (Figure 10b). As for LHS−Ni, the dehydration occurred via a topotactic process.

For LHS−Zn, the $\Delta\nu$ value remains almost constant upon dehydration, showing that the acetate anion acts as a free species intercalated between the layers. The interlamellar distance also remains almost constant upon heating. The total release of water at 110 °C led, via a destructive process, to the formation of an oxoacetate. These results indicate that LHS−Zn has a structural model closely related to the zinc hydroxynitrate form, with water occupying the fourth apex of the tetrahedron and the acetate anion intercalated between the layers (Figure 10c). Conversely, the LHS−Zn prepared by an exchange reaction[13] conserves the interlamellar organization of the starting material $Zn_5(OH)_8Cl_2 \cdot H_2O$, which is similar to that observed for LHS−M (M = Ni and Co). This clearly evidences the influence of the preparative route on the structural characteristics of such materials.

Conclusion

This work describes a new method for preparing layered hydroxyde acetates. This novel route, involving hydrolysis and inorganic polymerization in polyol media, offers several advantages compared to classical methods conducted in aqueous solution. It allows simple control of the reaction by means of the hydrolysis ratio rather than pH as in aqueous solution, avoids contamination with carbonate anion, and permits a rapid and easy process. The use of several techniques allows us to discuss in more detail the main characteristics of these poorly ordered compounds. Our comparative study

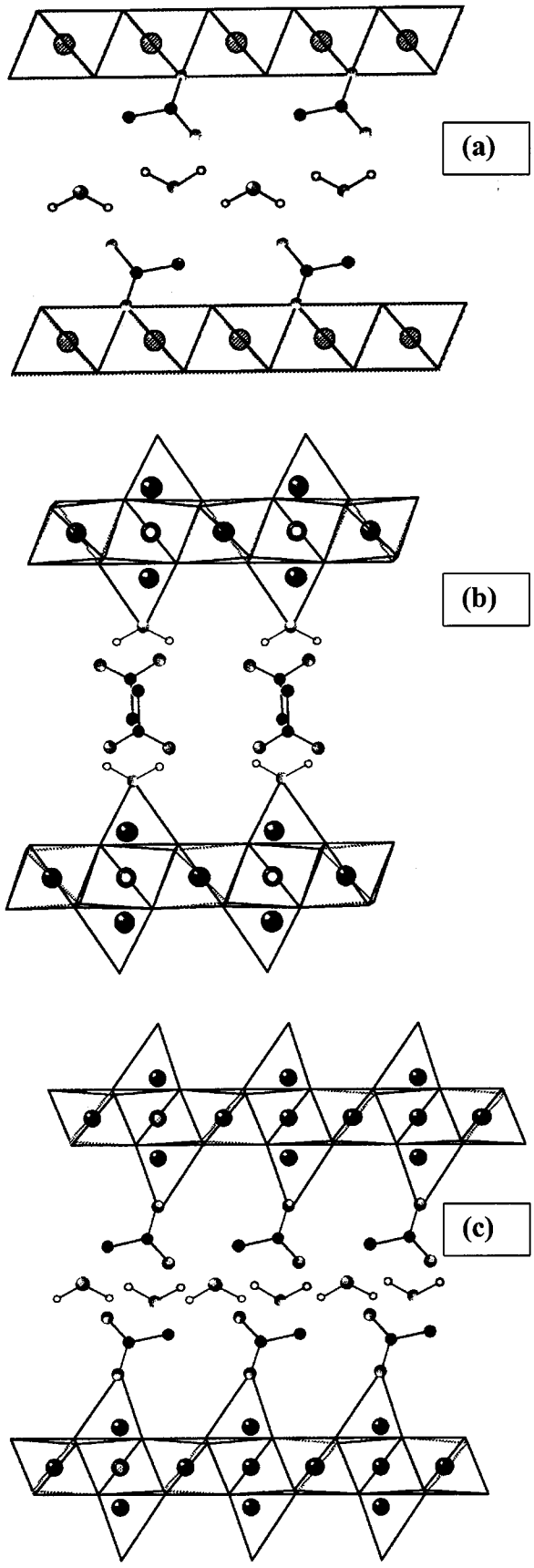

Figure 10. Structural model proposed for (a) LHS−Ni, (b) LHS−Co, and (c) LHS−Zn.

(47) Baddour, R.; Pereira-Ramos, J. P.; Messina R.; Perichon, J. *J. Electroanal. Chem.* **1991**, *314*, 81.

revealed significant differences, which concern mainly the nature of the cation site and the organization of water molecules and acetate anions between the layers. This organization is established for the first time. LHS−Ni and LHS−Co have a reversible topotactic dehydration process, which conserves their lamellar character. This process is of interest because it shows that these two materials can be handled in a relatively wide temperature range. Conversely, LHS−Zn undergoes a destructive dehydration process leading to ZnO.

Acknowledgment. We are deeply indebted to the Institut des Matériaux Jean Rouxel (IMN, Nantes, France) for the extensive use of some laboratory equipment. Special thanks are addressed to Dr. Y. Piffard for his interest in this work and for helpful discussions and to S. Grolleau for technical assistance. The authors also thank P. Gredin and J.-P. Souron from the Laboratoire de Cristallochimie du Solide, directed by Pr. M. Quarton, for temperature-resolved X-ray diffraction measurements. This work is dedicated to the memory of Professor Jean Rouxel.

CM991179J